

Functionalised staple linkages for modulating the cellular activity of stapled peptides

Yu Heng Lau,^a Peterson de Andrade,^a Soo-Tng Quah,^b Maxim Rossmann,^c Luca Laraia,^{a,f} Niklas Sköld,^a Tze Jing Sum,^a Pamela J. E. Rowling,^d Thomas L. Joseph,^e Chandra Verma,^e Marko Hyvönen,^c Laura S. Itzhaki,^d Ashok R. Venkitaraman,^f Christopher J. Brown,^b David P. Lane^b and David R. Spring^{a*}

^a University Chemical Laboratory, University of Cambridge, Lensfield Road, Cambridge CB2 1EW, United Kingdom

^b p53 laboratory (A*STAR), 8A Biomedical Grove, #06-04/05, Neuros/Immunos, Singapore 138648

^c Department of Biochemistry, University of Cambridge, 80 Tennis Court Road, Cambridge CB2 1GA, United Kingdom

^d Department of Pharmacology, University of Cambridge, Tennis Court Road, Cambridge CB2 1PD, United Kingdom

^e Bioinformatics Institute (A*STAR), 30 Biopolis Street, #07-01 Matrix, Singapore 138671; Department of Biological Sciences, National University of Singapore (NUS), Singapore 119077; School of Biological Sciences, Nanyang Technological University (NTU), Singapore 639798

^f MRC Cancer Unit, Hutchison/MRC Research Centre, Hills Road, Cambridge CB2 0XZ, United Kingdom

Supporting Information

1. General Experimental Details
2. Synthetic Procedures
3. NMR Spectra
4. Peptide Synthesis and Characterisation
5. Fluorescence Polarisation Assays
6. Isothermal Calorimetry
7. Molecular Dynamics Simulations
8. Confocal Microscopy
9. T22 Gene Reporter Assay
10. References

1. General Experimental Details

Imidazole-1-sulfonyl azide hydrochloride,¹ tris(3-hydroxypropyltriazolylmethyl)amine (THPTA),² 5-carboxytetramethylrhodamine (5-TAMRA)³ and 3,5-diethynylaniline⁴ were synthesised according to literature procedures. All other reagents were purchased from commercial sources and used without further purification. Tetrahydrofuran was dried over sodium wire and distilled from a mixture of calcium hydride and lithium aluminium hydride with triphenylmethane as indicator. Diethyl ether was distilled from a mixture of calcium hydride and lithium aluminium hydride. Dichloromethane, methanol, hexane, acetonitrile and toluene were distilled from CaH₂. Dimethylformamide (DMF) for peptide synthesis was purchased from Sigma-Aldrich. Petroleum ether (PE 40-60) refers to the fraction of petroleum with the boiling point range 40-60 °C. Reactions were carried out under dry nitrogen atmosphere at room temperature unless otherwise stated.

Thin layer chromatography was carried out on glass Merck Kieselgel 60 F254 plates, visualised by ultraviolet irradiation (254 and 365 nm) or ninhydrin (0.3% w/v in ethanol), prepared by standard procedures. Retention factors (R_f) are quoted to 0.01. Flash column chromatography was performed using Kieselgel 60 silica (230-400 mesh) with distilled solvents under a positive pressure of nitrogen.

¹H nuclear magnetic resonance spectra were recorded on Bruker Avance Ultrashield 400 or 500 spectrometers. Chemical shifts (δ) are quoted to the nearest 0.01 ppm and are referenced to the solvent residual peak. Coupling constants (J) are reported to the nearest 0.5 Hz. Data are reported as follows: chemical shift, multiplicity (br, broad; s, singlet; d, doublet; t, triplet; q, quartet; m, multiplet; or a combination of these), coupling constant(s), integration and assignment.

¹³C nuclear magnetic resonance spectra were recorded on Bruker Avance Ultrashield 400 or 500 spectrometers. Assignments are supported by DEPT-135, HSQC and HMBC spectra where necessary. Chemical shifts are quoted to the nearest 0.1 ppm and are referenced to the solvent residual peak. Quaternary carbons are reported as C_Q.

Infra-red spectra were recorded neat on a Perkin Elmer Spectrum One FT-IR spectrophotometer fitted with an attenuated total reflectance (ATR) sampling accessory. Absorption maxima are reported in wavenumbers (cm⁻¹).

Melting points were measured using a Büchi B545 melting point apparatus and are uncorrected.

Optical rotation was measured on a Perkin Elmer 343 polarimeter. $[\alpha]_D$ values are reported in 10⁻¹ deg cm² g⁻¹ at 589 nm, with concentration (c) given in g/100 mL.

High resolution mass spectrometry (HRMS) was carried out using a Waters LCT Premier Time of Flight mass spectrometer or Micromass Quadrupole-Time of Flight mass spectrometer. Reported mass values are within the error limits of ± 5 ppm.

Liquid chromatography-mass spectrometry (LCMS) was run on an Agilent 1200 series LC with an ESCi Multi-Mode Ionisation Waters ZQ spectrometer using MassLynx 4.1 software.

LC system: solvent A: 10 mM ammonium acetate + 0.1% formic acid in water; solvent B: 95% acetonitrile + 5% H₂O + 0.05% formic acid; column: Supelcosil ABZ+PLUS column (33 mm \times 4.6 mm, 3 μ m); gradient: 0.0-0.7 min: 0% B, 0.7-4.2 min: 0-100% B, 4.2-7.7 min: 100% B, 7.7-8.5 min: 100-0% B; DAD spectrum: 190 nm-600 nm, interval 2.0 nm, peak width 0.200 min).

Analytical HPLC was run on an Agilent 1260 Infinity using a Supelcosil ABZ+PLUS column (150 mm \times 4.6 mm, 3 μ m) eluting with a linear gradient system (solvent A: 0.05% (v/v) TFA in water, solvent B:

0.05% (v/v) TFA in acetonitrile) over 15 min at a flow rate of 1 mL/min. Semi-preparative HPLC was run on an Agilent 1260 Infinity using a Supelcosil ABZ+PLUS column (250 mm × 21.2 mm, 5 μm) eluting with a linear gradient system (solvent A: 0.1% (v/v) TFA in water, solvent B: 0.05% (v/v) TFA in acetonitrile) over 20 min at a flow rate of 20 mL/min. HPLC was monitored by UV absorbance at 220 and 254 nm, with TAMRA-labelled peptides also monitored at 550 nm. Retention times (t_r) are reported to the nearest 0.01 min.

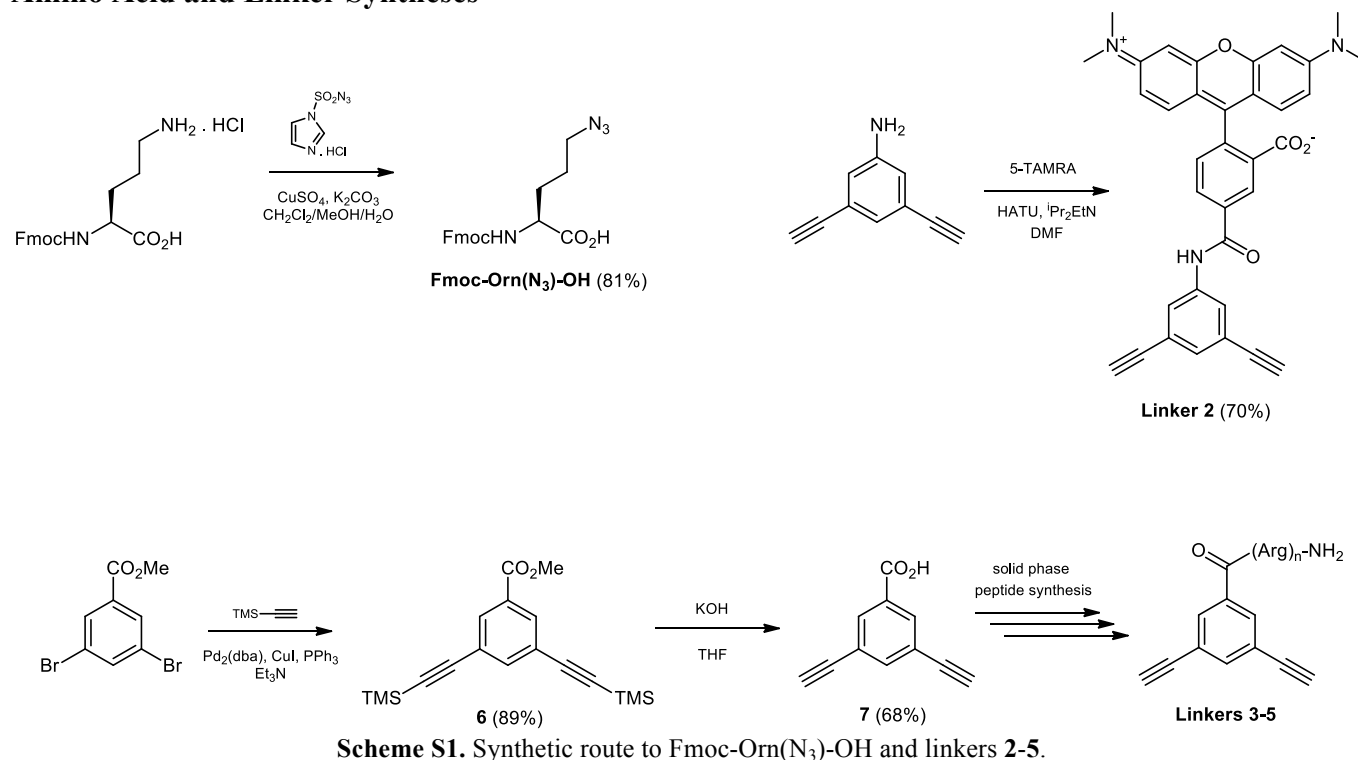
Peptide concentrations were determined by amino acid analysis at the Peptide Nucleic Acid Chemistry Facility at the Department of Biochemistry, University of Cambridge.

2. Synthetic Procedures

General Peptide Stapling Protocol

A solution of diazido peptide (1 equiv) and dialkynyl linker (1.1 equiv) in 1:1 *tert*-butanol/water (1 mL/mg peptide) was degassed with nitrogen for 15 min, followed by the addition of copper(II) sulfate pentahydrate (1 equiv), tris(3-hydroxypropyltriazolylmethyl)amine (1 equiv) and sodium ascorbate (3 equiv). After stirring under nitrogen at rt for 16 h, the reaction mixture was lyophilised and purified by HPLC to give the final stapled peptide.

Amino Acid and Linker Syntheses



Fmoc-Orn(N₃)-OH

Fmoc-Orn-OH.HCl (1.0162 g, 2.60 mmol) was dissolved in a biphasic mixture of water (15 mL), methanol (30 mL) and dichloromethane (25 mL). Copper(II) sulfate pentahydrate (5.0 mg, 0.020 mmol) and imidazole-1-sulfonyl azide hydrochloride (2.00 g, 9.54 mmol) were added, and the mixture was adjusted to pH 9 with aqueous potassium carbonate solution. After stirring vigorously for 18 h, the organic solvents were removed *in vacuo*. The remaining aqueous phase was washed with diethyl ether (2 × 20 mL), acidified to pH 2 with concentrated hydrochloric acid and extracted with diethyl ether (3 × 30 mL). The organic extracts were dried over magnesium sulfate and concentrated *in vacuo*. The oily residue was redissolved in dichloromethane (10 mL), then the solvent was removed under a stream of nitrogen to give the azido amino acid Fmoc-Orn(N₃)-OH (805 mg, 81%) as a white amorphous solid.

m.p. 132-134 °C. IR (ATR): 3300-2800 (br, O-H), 2096 (N₃), 1718 (C=O), 1524, 1451, 1249, 1079, 741 cm⁻¹. ¹H NMR (400 MHz, CDCl₃): δ = 7.77 (d, 2H, *J* = 7.5 Hz, ArH), 7.59 (m, 2H, ArH), 7.41 (t, 2H, *J* = 7.5 Hz, ArH), 7.32 (tt, 2H, *J* = 7.5, 1.1 Hz, ArH), 5.31 (d, 1H, *J* = 8.0 Hz, CONH), 4.66-4.36 (m, 3H, α-CH and OCH₂), 4.22 (t, 1H, *J* = 6.5 Hz, fluorenyl 9-H), 3.40-3.08 (m, 2H, δ-CH₂), 2.08-1.37 (m, 4H, β- and γ-CH₂). ¹³C NMR (100 MHz, CDCl₃): δ = 176.2 (CO₂H), 156.2 (CONH), 143.9 (2 × C_QAr), 143.7 (C_QAr), 141.5 (C_QAr), 127.9 (2 × CHAr), 127.2 (2 × CHAr), 125.2 (2 × CHAr), 120.2 (2 × CHAr), 67.3 (OCH₂), 53.3 (α-CH), 50.9 (δ-CH₂), 47.3 (fluorenyl C-9), 29.8 (β-CH₂), 25.0 (γ-CH₂). HRMS (ES⁺): *m/z* [M+H]⁺ calcd for C₂₀H₂₁N₄O₄: 381.1563; found: 381.1565.

Characterisation data is in accordance with that previously reported.⁵

Linker 2.

A solution of 5-TAMRA (187 mg, 0.435 mmol) and *N,N*-diisopropylethylamine (123 μ L, 0.708 mmol) in DMF (10 ml) was pre-activated by the addition of HATU (129 mg, 0.339 mmol) for 15 min, followed by the addition of diethynylaniline (54.0 mg, 0.383 mmol). After stirring for 16 h, the solvent was removed *in vacuo* and the crude residue was purified by column chromatography (5-15% methanol in dichloromethane) to give linker **2** (148 mg, 70%) as a dark red-purple solid.

R_f (20% MeOH in CH_2Cl_2) = 0.54. IR (ATR): 3273 (C–H), 2923 (C–H), 1712 (C=O), 1651, 1651 (C=O), 1592, 1490, 1407, 1343, 1185, 1125 cm^{-1} .

^1H NMR (400 MHz, $(\text{CD}_3)_2\text{SO}$): δ = 10.76 (s, 1H, NH), 8.74 (br s, 1H, TAMRA 3-H), 8.39 (d, 1H, J = 7.5 Hz, TAMRA 5-H), 8.01 (d, 2H, J = 1.5 Hz, CHAr), 7.60 (br s, 1H, TAMRA 6-H), 7.35 (t, 1H, J = 1.5 Hz, CHAr), 7.23-6.60 (m, 6H, TAMRA 1,2,4,5,7,8-H), 4.32 (s, 2H, $\text{C}\equiv\text{CH}$), 3.20 (br s, 1H, CH_3). ^{13}C NMR (125 MHz, $(\text{CD}_3)_2\text{SO}$ + 40% NaOD in D_2O): δ = 168.3 (CO_2H), 164.4 (CONH), 155.4 (TAMRA C-1), 152.2 (two of TAMRA C3',4a',6',10a'), 152.0 (two of TAMRA C3',4a',6',10a'), 139.6 (CONHC_Q), 136.0 (TAMRA C-4), 135.0 (TAMRA C-5), 129.8 (CHAr), 128.4 (TAMRA C-1',8'), 126.9 (TAMRA C-2), 124.5 (TAMRA C-6), 123.7 (TAMRA C-3 or 2 \times CHAr), 123.6 (TAMRA C-3 or 2 \times CHAr), 122.7 (2 \times C_QC \equiv CH), 109.1 (TAMRA C-2',7'), 105.4 (TAMRA 8a',9a'), 98.0 (TAMRA 4',5'), 85.0 (TAMRA C-9), 82.3 (2 \times C \equiv CH), 81.7 (2 \times C \equiv CH), 39.5 (4 \times CH_3 , overlapping with solvent residual peak). HRMS (ES⁺): m/z [M+H]⁺ calcd for $\text{C}_{35}\text{H}_{27}\text{N}_3\text{O}_4$: 554.2074; found: 554.2085.

Methyl 3,5-bis((trimethylsilyl)ethynyl)benzoate (6).

Methyl 3,5-dibromobenzoate (1.52 g, 5.17 mmol), tris(dibenzylideneacetone)dipalladium(0) (90 mg, 0.098 mmol), copper(I) iodide (19 mg, 0.10 mmol) and triphenylphosphine (129 mg, 0.492 mmol) were added to dry distilled triethylamine (25 mL), followed by trimethylsilylacetylene (10 mL, 70.3 mmol). After stirring at 65 $^\circ\text{C}$ overnight, the reaction mixture was concentrated *in vacuo* and the crude residue was purified by column chromatography (1% ethyl acetate in PE 40-60) to give the product **6** (1.52 g, 89%) as a dark yellow solid.

R_f (1% ethyl acetate in PE 40-60) = 0.44. m.p. 71-73 $^\circ\text{C}$. IR (ATR): 2956 (CH), 2158 (C \equiv C), 1733 (C=O), 1439, 1320, 1250, 1228, 843 cm^{-1} . ^1H NMR (500 MHz, CDCl_3): δ = 8.04 (d, J = 1.5 Hz, 2H, ArH), 7.72 (t, J = 1.5 Hz, 1H, ArH), 3.91 (s, 3H, CH_3), 0.24 (s, 18H, $\text{Si}(\text{CH}_3)_3$). ^{13}C NMR (125 MHz, CDCl_3): δ = 165.8 (C=O), 139.2 (CHAr), 132.8 (2 \times CHAr), 130.7 (C_QAr), 124.0 (2 \times C_QAr), 103.1 (2 \times C \equiv C–TMS), 96.3 (2 \times C \equiv C–TMS), 52.6 (OCH₃), 0.0 (2 \times $\text{Si}(\text{CH}_3)_3$). LCMS (AP⁺): m/z 328.97 ([M+H]⁺, t_r = 6.0 min).

Characterisation data is in accordance with that previously reported.⁶

3,5-Diethynylbenzoic acid (7).

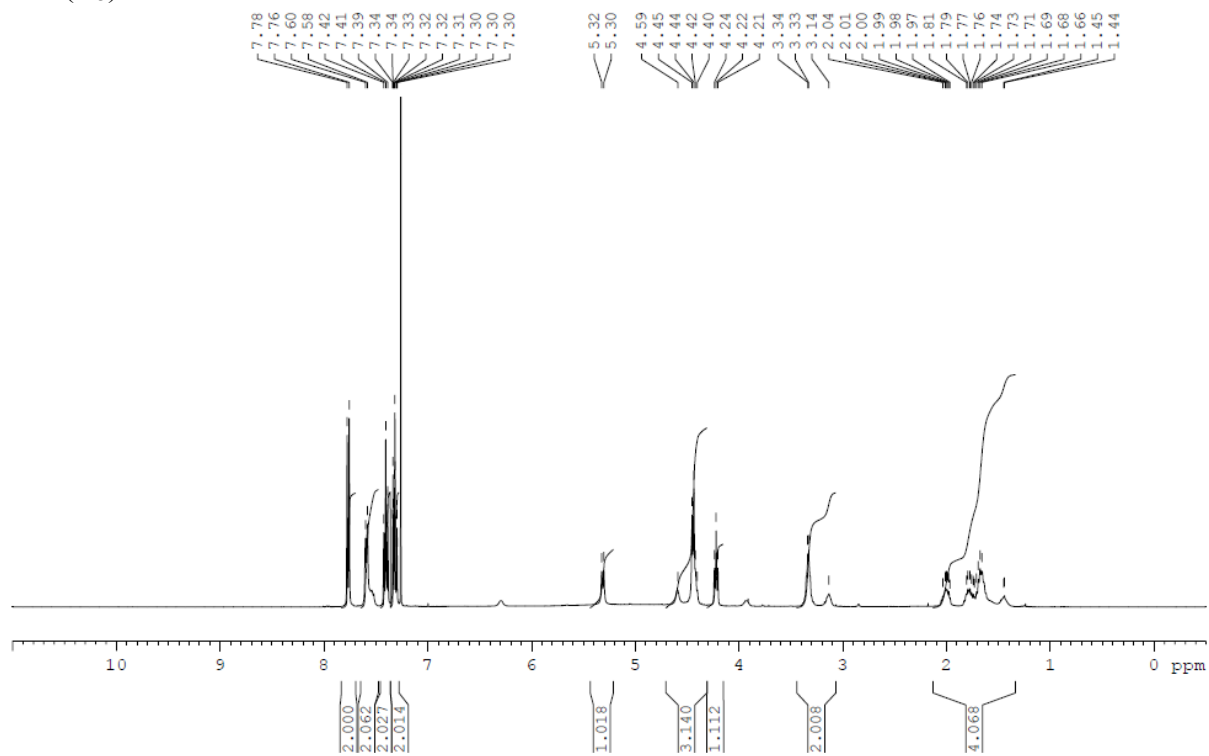
Aqueous 6M potassium hydroxide solution (2.50 mL, 15.0 mmol) was added to a solution of **6** (850 mg, 2.59 mmol) in tetrahydrofuran (15 mL). After stirring for 16 h, the volatile solvents were removed *in vacuo*. The remaining aqueous mixture was acidified with 2M hydrochloric acid (40 mL) and extracted with diethyl ether (3 \times 40 mL). The combined organic extracts were dried over magnesium sulfate and concentrated *in vacuo*. The crude product was recrystallised from chloroform to give the pure product **7** as a pale brown solid (298 mg, 68%).

m.p. 250 $^\circ\text{C}$ decomp. (lit. m.p. 173 $^\circ\text{C}$;⁸ 283 $^\circ\text{C}$ decomp.⁹). IR (ATR): 3286 (OH), 1682 (C=O), 1589, 1444, 1311, 1241, 900, 670 cm^{-1} . ^1H NMR (500 MHz, CDCl_3): δ = 8.18 (d, J = 1.5 Hz, 2H, ArH), 7.81 (t, J = 1.5 Hz, 1H, ArH), 3.16 (s, 2H, C \equiv CH). ^{13}C NMR (125 MHz, CDCl_3): δ = 169.5 (CO_2H), 140.2 (2 \times CHAr), 133.9 (CHAr), 130.0 (C_QAr), 123.4 (2 \times C_QAr), 81.5 (2 \times C \equiv C–H), 79.3 (2 \times C \equiv C–H). LCMS (ES⁻): m/z 169.1 ([M–H]⁻, t_r = 4.2 min)

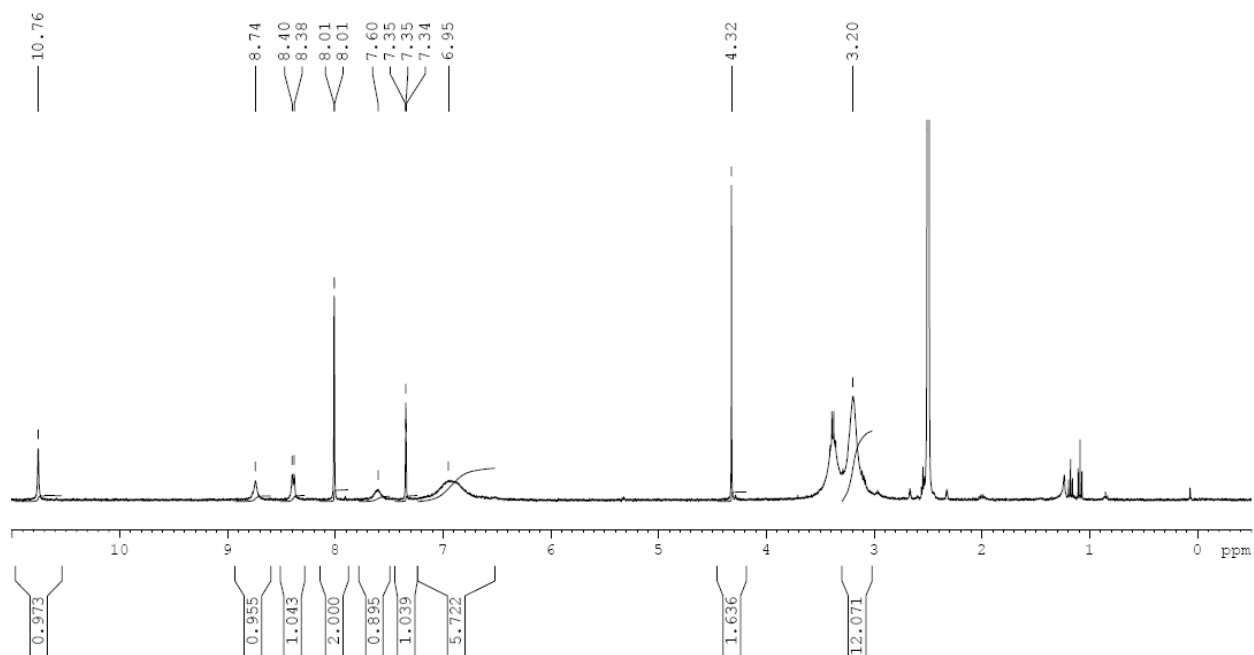
Characterisation data is in accordance with that previously reported.^{7,8}

3. NMR Spectra

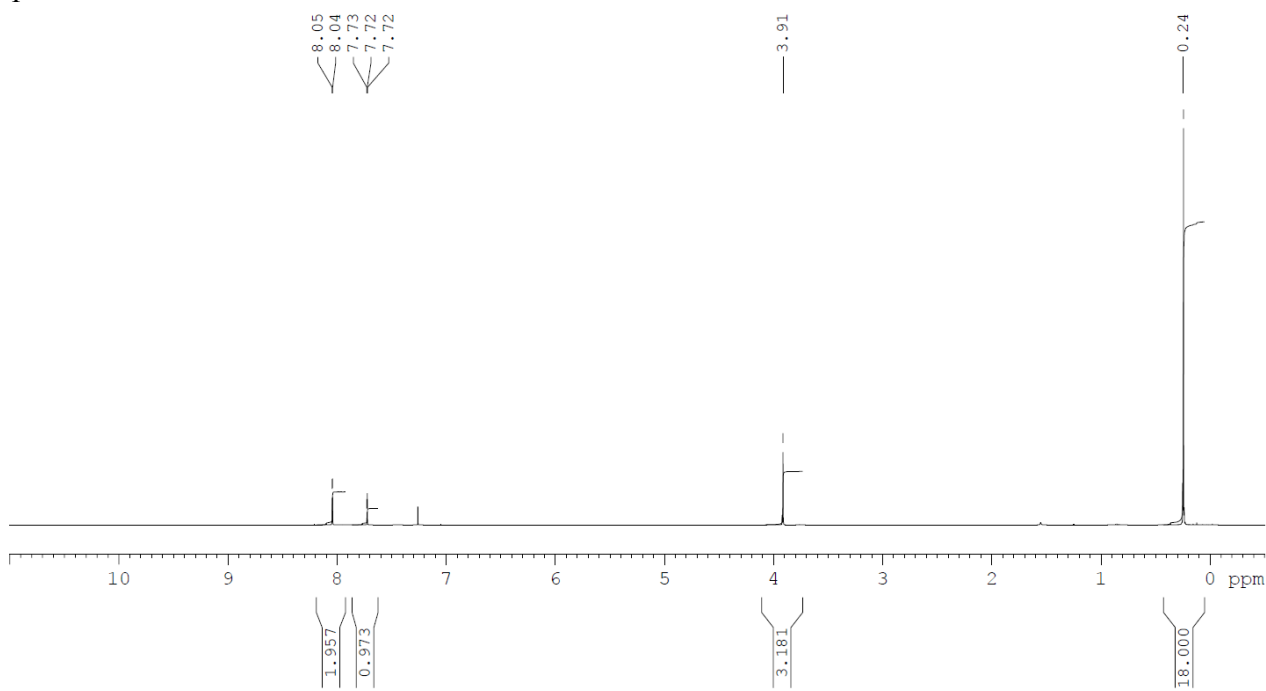
Fmoc-Orn(N₃)-OH



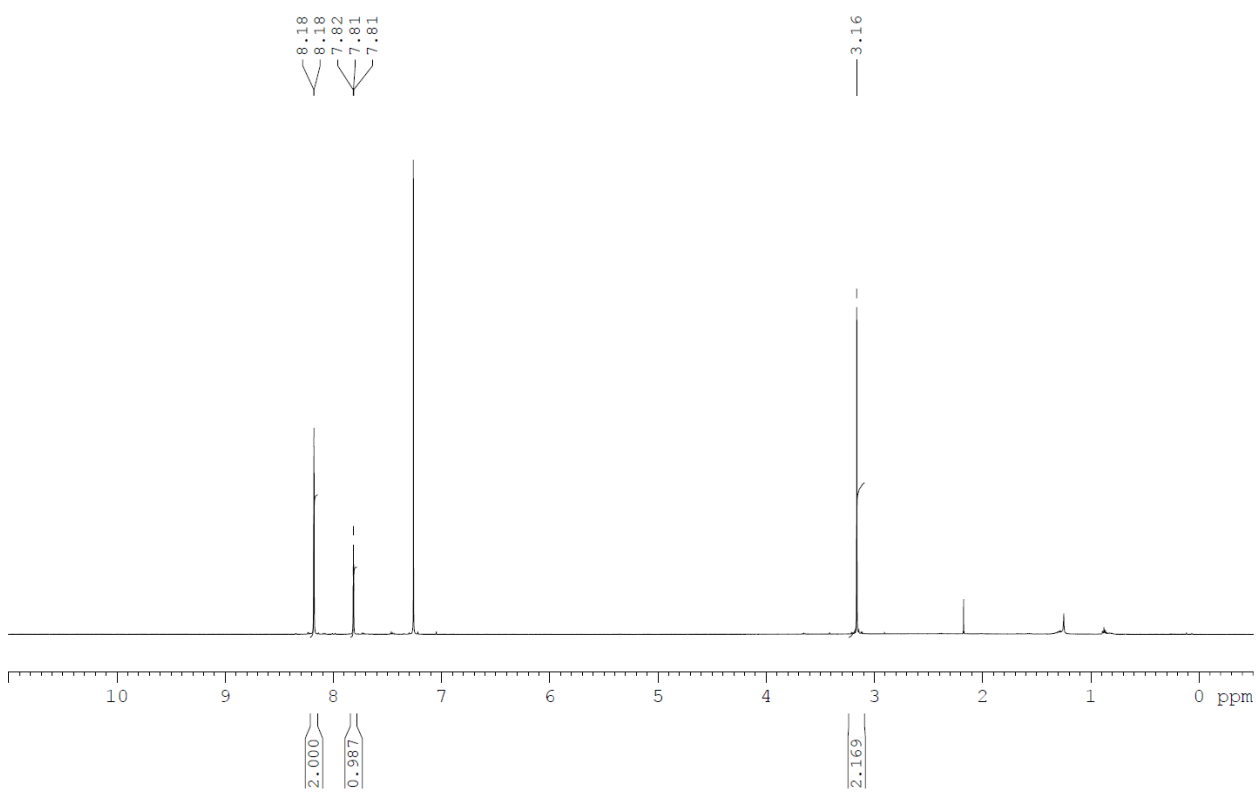
Linker 2



Compound 6



Compound 7



4. Peptide Synthesis and Characterisation

4.1 Fmoc Solid-Phase Peptide Synthesis

Manual peptide synthesis was performed on Novabiochem Rink Amide MBHA resin (0.52 mmol/g loading). Couplings were carried out by adding diisopropylcarbodiimide (4 equiv) to a solution of the Fmoc-protected amino acid (4 equiv) in DMF (~0.4 M). After 10 s, the mixture was added to ethyl cyanoglyoxylate 2-oxime (4 equiv). This pre-activated mixture was then added to the resin in DMF and shaken for 1 h. The side chain protecting groups used were *t*-Bu for aspartic acid, glutamic acid, serine, threonine, Boc for lysine and tryptophan, Pbf for arginine, and Trt for asparagine.

N-terminal capping with 5-TAMRA and compound **7** were carried out in a similar manner, pre-activating the carboxylic acid (6 equiv) with diisopropylcarbodiimide (6 equiv) and ethyl cyanoglyoxylate 2-oxime (6 equiv) followed by addition to the resin in DMF and shaking for 3 h in the case of 5-TAMRA, and 1 h in the case of compound **7**. N-terminal acetyl capping was carried out by treating resin swelled in dichloromethane with acetic anhydride (10 equiv) and *N,N*-diisopropylethylamine (10 equiv) for 1.5 h.

Completion of peptide couplings was determined by a chloranil test, in which acetaldehyde (200 μ L) and a saturated solution of chloranil in toluene (50 μ L) were added to a small amount of resin swelled in dichloromethane. After five minutes shaking at rt, no change in colour indicated complete coupling, whilst green colouration of the resin indicated incomplete coupling. Any incomplete couplings were submitted to a second round of coupling.

Fmoc deprotection was carried out with 20% piperidine in DMF (1 \times 1 min, 2 \times 10 min). Cleavage from the resin was achieved with 2.5% triisopropylsilane and 2.5% dichloromethane and 2.5% water in TFA for 2 h. The solvent was removed under a stream of nitrogen and the residue triturated with diethyl ether (3 \times 5 mL) before purification by HPLC.

In the case of arginine linkers **3-5**, the purity was sufficient after cleavage and trituration to be used for stapling without further purification.

4.2 Peptide LCMS Data

Table S1. Peptide sequences and LCMS data. Calculated m/z ratios are for $[M+2H]^{2+}$ unless otherwise specified.

Peptide Name	Peptide Sequence	Mass	m/z found	m/z calcd
p 53 ₍₁₇₋₂₉₎	Ac-ETFSDLWKLLPEN-NH ₂	1631.82	817.34	817.42
SP 0	Ac-ETF-Orn(N ₃)-DLWRL-Orn(N ₃)-EN-NH ₂	1755.88	879.9	879.95
SP 1	SP 0 + Linker 1	1881.93	943.2	942.97
SP 2	SP 0 + Linker 2	2309.08	1156.26	1156.05
SP 3	SP 0 + Linker 3	2081.03	1042.05	1042.02
SP 4	SP 0 + Linker 4	2237.14	1120.27	1120.07
SP 5	SP 0 + Linker 5	2393.24	1198.33	1198.13
RRR-SP 0	Ac-RRRETFSDLWRL-Orn(N ₃)-EN-NH ₂	2224.18	1113.90	1113.60
TAMRA-p 53 ₍₁₇₋₂₉₎	TAMRA-Ahx-ETFSDLWKLLPEN-NH ₂	2115.04	1059.15	1059.02
TAMRA-SP 0	TAMRA-Ahx-ETF-Orn(N ₃)-DLWRL-Orn(N ₃)-EN-NH ₂	2239.1	1143.14	1143.04 [M+2Na] ²⁺
TAMRA-SP 1	TAMRA-SP 0 + Linker 1	2365.14	1184.08	1184.08
TAMRA-SP 3	TAMRA-SP 0 + Linker 3	2564.25	856.19	856.09 [M+3H] ³⁺

TAMRA-SP4	TAMRA-SP0 + Linker 4	2720.35	908.32	908.46 [M+3H] ³⁺
TAMRA-SP5	TAMRA-SP0 + Linker 5	2876.45	960.38	960.49 [M+3H] ³⁺
3	Compound 7-Arg-NH ₂	325.15	326.06	326.16 [M+H] ⁺
4	Compound 7-(Arg) ₂ -NH ₂	481.25	241.63	241.63
5	Compound 7-(Arg) ₃ -NH ₂	637.36	319.62	319.68
FP tracer	TAMRA-RFMDYWEGL-NH ₂	1626.70	814.43	814.35

4.3 Example HPLC Chromatographs of Crude Stapling Reaction Mixture

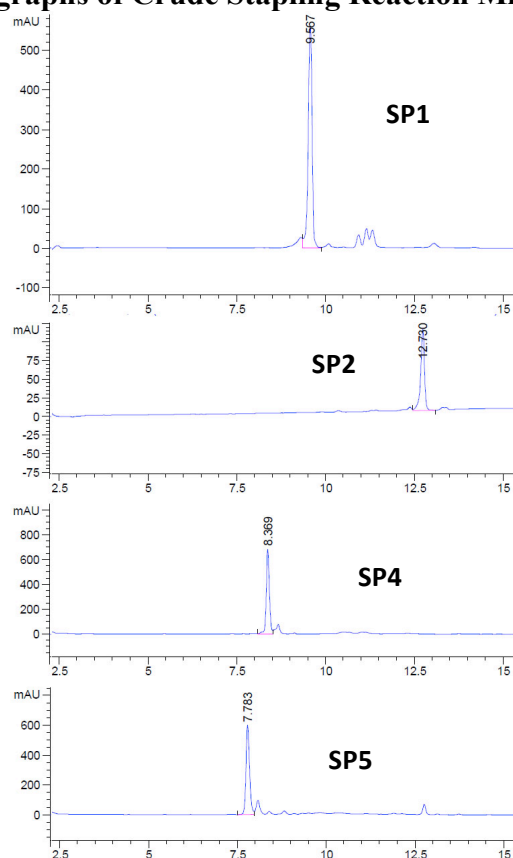


Figure S1. HPLC chromatographs of crude reaction mixtures for the stapling reaction to give (top to bottom): **SP1**, **SP2**, **SP4** and **SP5**, monitored at 220 nm.

4.4 Confirming the Formation of Stapled Peptides

To confirm that the products being formed were not linear coupling products of the same mass, we searched for the presence of a free unreacted azido group. The infra-red spectra (Figure S2) at $\sim 2100\text{ cm}^{-1}$ confirmed the absence of azides in the stapled products, with the unstapled peptide as a positive control (azides present) and native p53 sequence (no azides present) as a negative control.

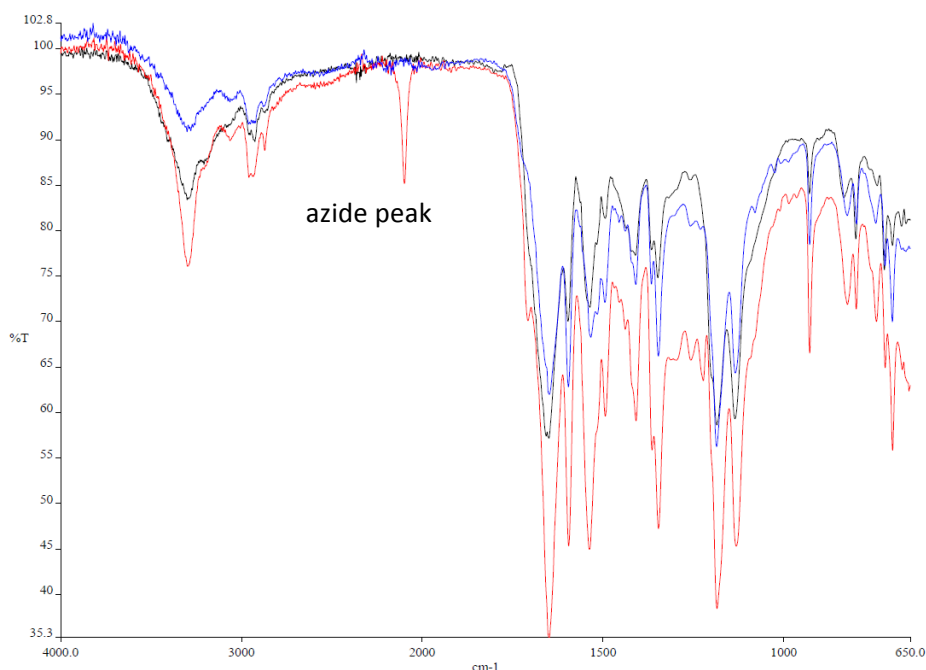


Figure S2. Infra-red spectra of TAMRA-SP5 (black), TAMRA-SP0 (red) and TAMRA-p53₍₁₇₋₂₉₎ (blue). Only the spectrum of the unstapled peptide contains a peak at ~2100 cm⁻¹ for azides.

Furthermore, the stapled products were unreactive to an excess of sacrificial alkyne (eg. propargylamine) under Cu-catalysed azide-alkyne cycloaddition conditions.

To eliminate the possibility of higher order oligomers with the same m/z ratio being formed, high resolution mass spectra were obtained (Figure S3), showing the expected isotopic spacing for the monomeric stapled product.

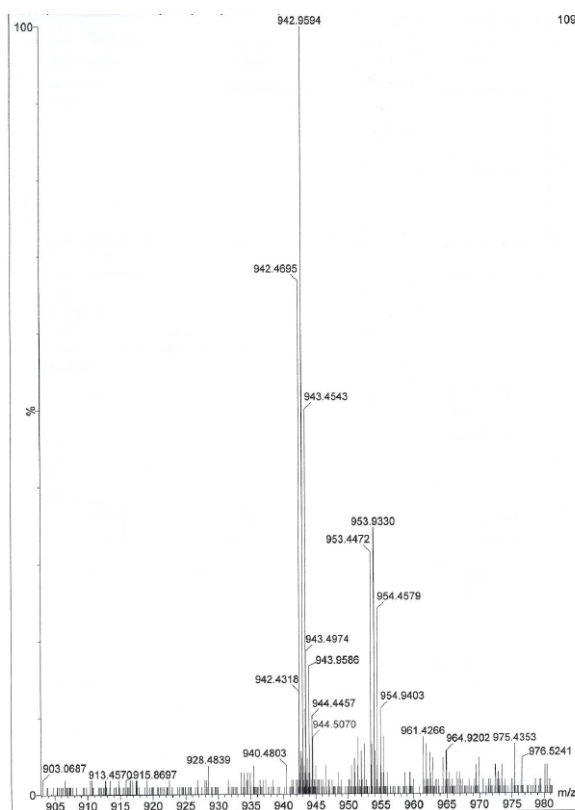


Figure S3. Mass chromatogram of SPI showing the isotope peaks for $[M+2H]^{2+}$ separated by ~0.5 amu, corresponding to peptides containing different numbers of the ¹³C isotope.

4.5 Circular Dichroism

Circular dichroism spectra (Figure S4) were obtained on a Chirascan CD spectrometer at 20 °C using a 1 mm path length, scanning between 260 and 195 nm at 0.2 nm/s with a bandwidth of 1.0 nm and response time of 0.5 s. Each spectrum is the average of three scans. Peptides were dissolved in 85:15 water/acetonitrile, with accurate concentrations determined by amino acid analysis. Helicity was calculated based on mean residue ellipticity at 222 nm as previously reported (Table S2).⁹

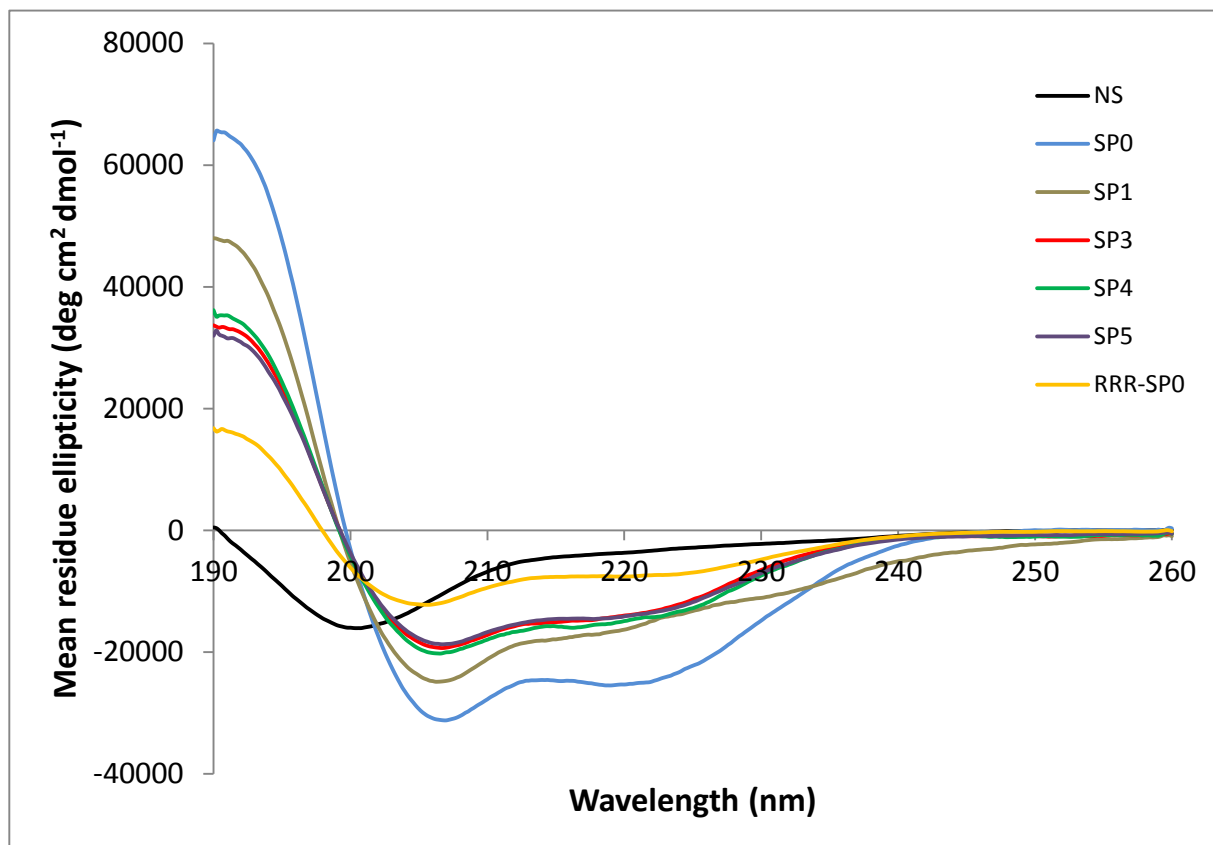


Figure S4. Circular dichroism spectra of peptides, showing that both the unstapled and stapled peptide are more helical than the native p53 sequence.

Table S2. Calculated helicity of unstapled and stapled peptides, based on mean residue ellipticity at 222 nm.

Peptide	Helicity (%)
p53 ₍₁₇₋₂₉₎	10
SP0	76
SP1	45
SP3	41
SP4	43
SP5	41
RRR-SP0	22

4.6 Serum Stability Assay

TAMRA-labelled peptide was dissolved in DMSO, then 5 µL was added to 500 µL of mouse serum (Sigma). 5-TAMRA was used as an internal standard. The mixture was incubated at 37 °C over 30 h, with 30 µL aliquots removed at various time points. Aliquots were immediately diluted with 30 µL acetonitrile, centrifuged, and the supernatant analysed by analytical HPLC, comparing the integration of the peptide peak against the internal standard at 550 nm (Figure S5). Experiments were done in duplicate.

5. Fluorescence Polarisation Assays

Overexpression and purification of MDM2

The p53-interacting domain of human MDM2 (amino acid residues 1-125) was expressed and purified following a literature procedures.¹⁰ The plasmid containing MDM2, kindly provided by Professor Sir Alan Fersht, was introduced into *E. coli* C41 cells.¹¹ Colonies were grown in 2TY media containing ampicillin (50 µg/mL) at 37°C, then induced overnight at an A_{600} of 0.6 with 0.5mM IPTG at 25°C. The cells were pelleted and resuspended in ice-cold buffer A (50 mM Tris-HCl (pH 8.0), 500 mM NaCl, 5 mM DTT, 1 mM EDTA, 0.1% (v/v) Triton X-100, EDTA-free protease inhibitors (Roche)) and lysed on a Emulsiflex C5 homogeniser (Glen Creston). The supernatant of the subsequent centrifugation of the cell lysate was bound onto Glutathione Sepharose 4B beads (GE Healthcare Life Sciences) for 1h at 4°C. The beads were washed with buffer B (buffer A without Triton X-100 and protease inhibitors) then eluted with reduced glutathione (3 × 15 mL, 10 mM). The eluted washings were cleaved with thrombin (250 units) overnight at rt. The cleavage mixture was purified on a size-exclusion gel-filtration column (HiLoad 16/60 Superdex G75), using PBS with DTT (2 mM) as the eluting solvent. Purified protein was flash-frozen and stored at -80°C until further use. Mass spectrometry of the protein gave the expected mass of 14.2 kDa. Protein composition and concentration was confirmed by amino acid analysis.

Fluorescence Polarisation Assays

Direct FP:

A stock solution of TAMRA-labelled peptide in DMSO (10 mM) was diluted in assay buffer to a concentration of 100 nM. MDM2 stock solution was diluted in assay buffer (1 × PBS + 0.01% Tween 20 + 3% DMSO) to a top concentration of 4 µM, then 1.6-fold serial dilutions were made to give a 16-point dose-response curve.

Peptide (20 µL) and MDM2 dilutions (20 µL) were added to a 384-well plate (Corning 3820 Assay Plate, 384 Well, Low volume, Flat Bottom, Black, Non-Binding Surface) and incubated at room temperature for 1h. The negative control was using assay buffer in place of MDM2. Experiments were conducted in two independent experiments, each in triplicate.

Fluorescence polarisation was measured using a BMG PHERAstar Plus plate reader. K_d values were calculated in GraphPad Prism software using a non-linear least squares analysis, fitting to the equation we have previously described and quoted with the standard error (Figure S5).¹²

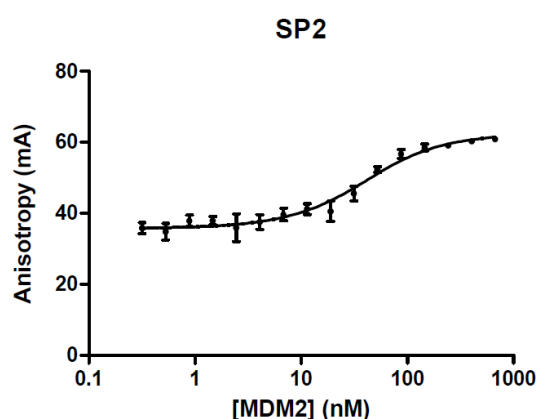


Figure S5. Direct FP titration curve for TAMRA-labelled peptide SP2 with MDM2.

Competitive FP:

This assay was based on an assay we previously described in the literature,¹² with a change in fluorophore on the FP tracer from 5-FAM to 5-TAMRA.

Stock solutions of peptides in DMSO (10 mM) were diluted in assay buffer (1 × PBS + 0.01% Tween 20

+ 3% DMSO) to a top concentration of 10 μ M, then 1.6-fold serial dilutions were made to give a 16-point dose-response curve. A stock solution of FP tracer (10 mM) in DMSO was diluted in assay buffer to a concentration of 200 nM (final assay concentration of 50 nM). MDM2 was diluted in assay buffer to a concentration of 380 nM (final assay concentration of 95 nM).

Dilutions of peptides (20 μ L), FP tracer (10 μ L) and MDM2 (10 μ L) were added to a 384-well plate and incubated at 4 °C for 1h. The negative controls used assay buffer in place of peptide, whilst the positive control was assay buffer in place of MDM2 and peptide. Experiments were conducted in two independent experiments, each in triplicate.

Fluorescence polarisation was measured using a BMG PHERAstar Plus plate reader. IC₅₀ values were calculated in GraphPad Prism software using a non-linear least squares analysis (Figure S6), whilst K_i values were calculated by using a non-linear least squares analysis fitting to the equations we have previously described for binding with receptor depletion, and quoted with the standard error.¹²

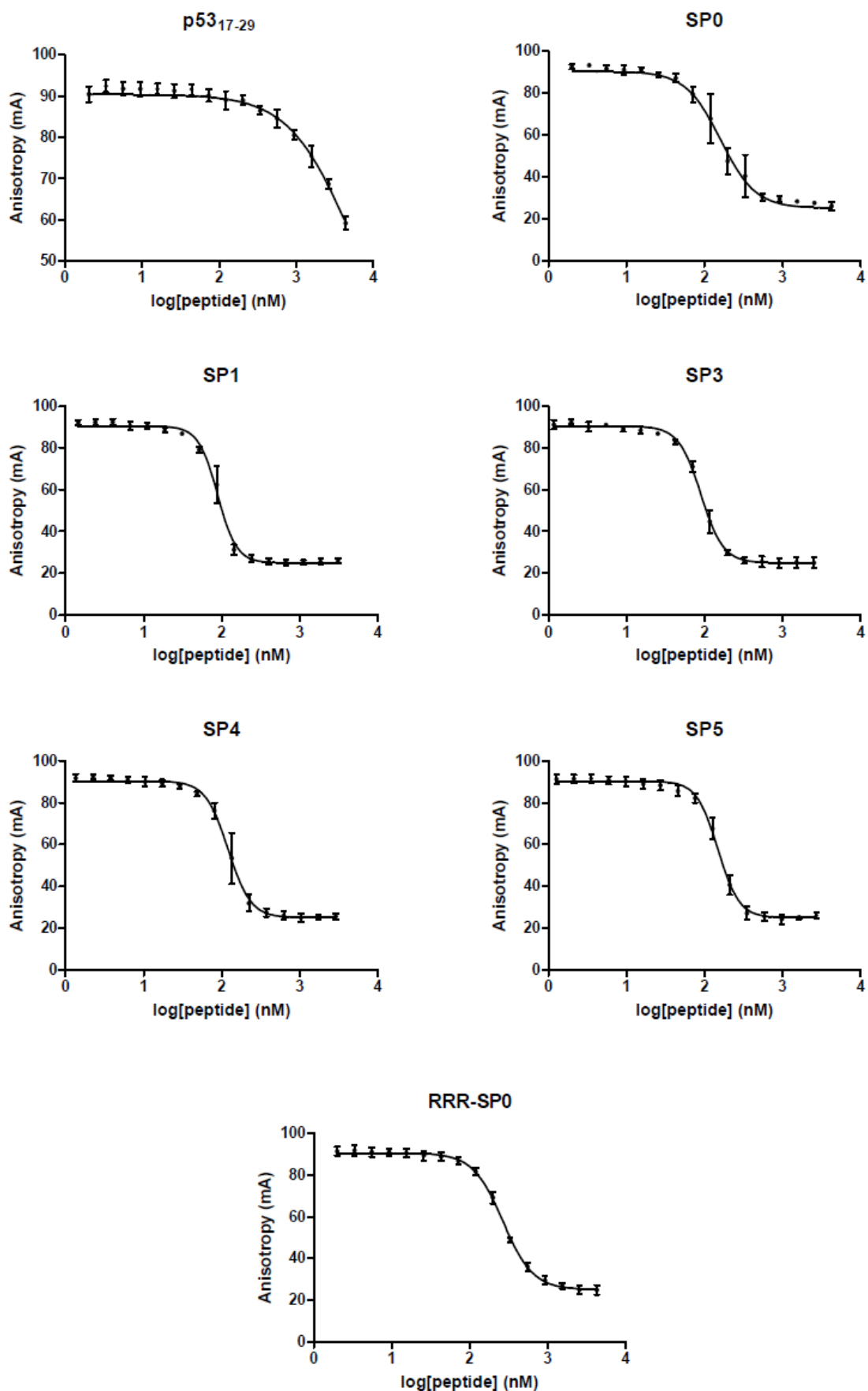


Figure S6. Competitive FP inhibition curves for peptides.

The FP tracer peptide was titrated with MDM2 in a direct fluorescence polarisation assay (Figure S7), and the K_d value was calculated to be 17.6 ± 1.7 nM.

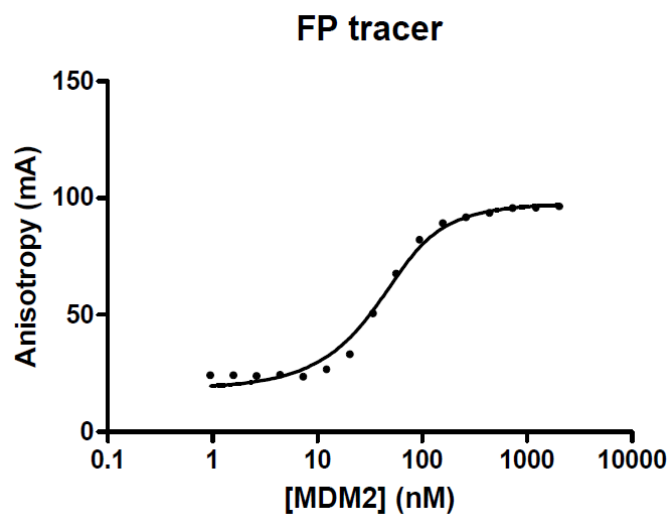


Figure S7. Direct titration of FP tracer with MDM2.

The Z-factor for the competitive FP assay was calculated to be 0.84 (Figure S8), based on 16 replicates of negative control (FP tracer, MDM2 and water) and positive control (FP tracer, assay buffer and water).

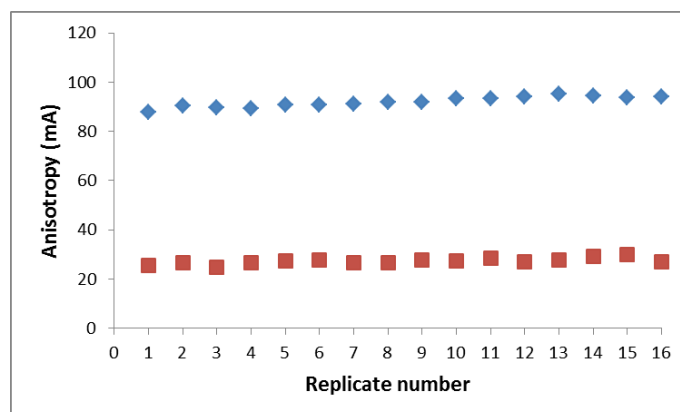


Figure S8. Replicates of positive (red) and negative control (blue) for competitive FP assay Z-score calculation.

6. Isothermal Calorimetry

Calorimetric titrations were performed on an ITC200 (MicroCal, Inc.) device. Proteins and peptides were buffer exchanged into 50 mM Na₂HPO₄, 10 mM KH₂PO₄, pH 7.4, 137 mM NaCl, 2.7 mM KCl, 0.5 μM TCEP, 0.05 % P20 buffer, 1% DMSO. The titration experiments were performed at 20 °C with an initial 0.4 μl injection at a duration of 0.8 s, followed by 19 2-μl injections at a duration of 4 s with 120 s spacing. For the binding assays 70 or 80 μM peptide was titrated into 7 – 8 μM MDM2 protein solution. Binding isotherms were fit by non-linear regression using the single-site model provided by Origin software (MicroCal, Inc.). The stoichiometry of the interaction (N), equilibrium association constant (K_a) and change of enthalpy (ΔH) were floated during the fitting.

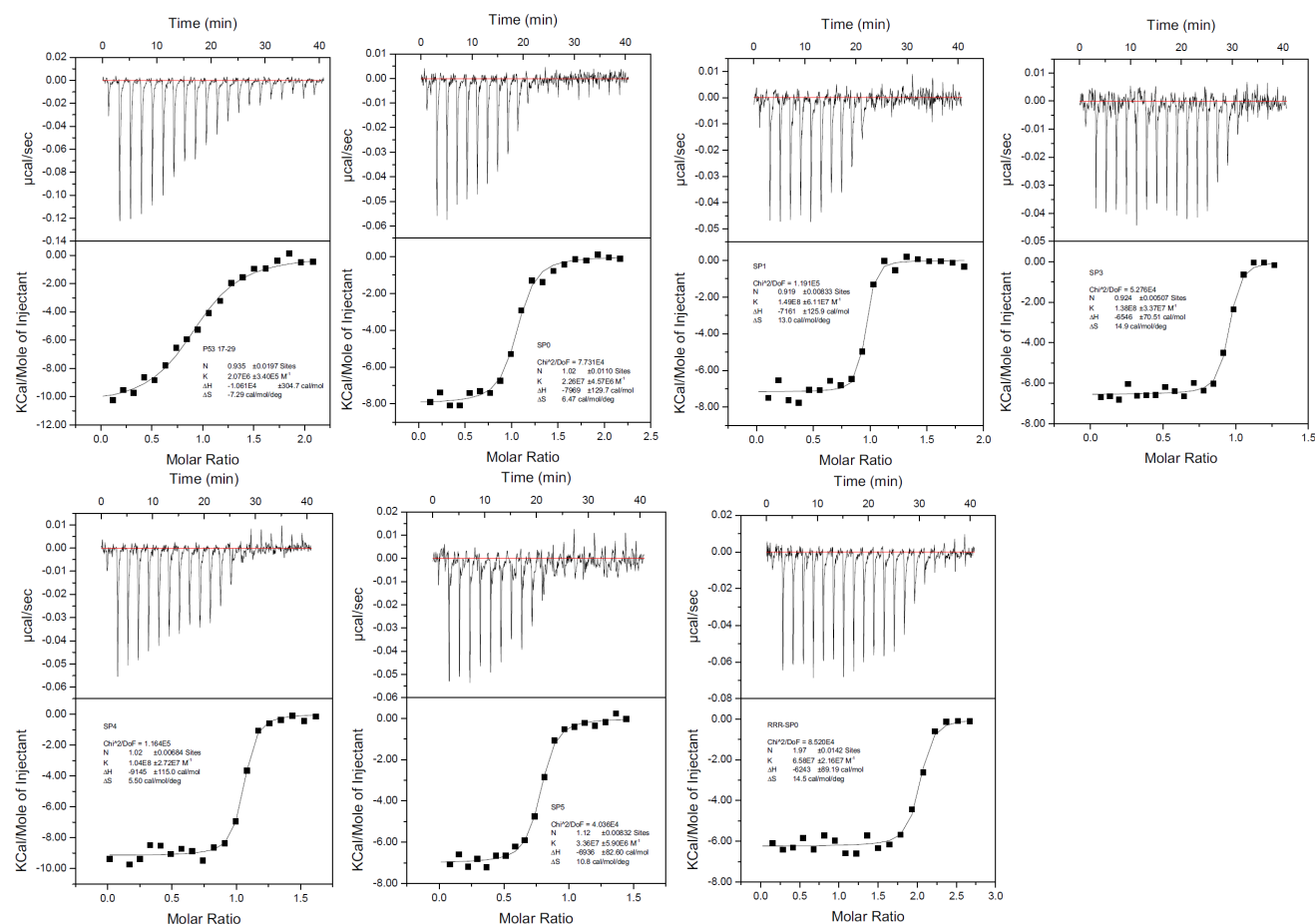


Figure S9. ITC data for p53₁₇₋₂₉, SP0, SP1, SP3 (top row left to right), and SP4, SP5 and RRR-SP0 (bottom row left to right).

7. Molecular Dynamics Simulations

The peptide sequence for stapling was based on the p53₍₁₇₋₂₉₎ sequence, using the K24R mutant to avoid ubiquitination as suggested by Verdine and coworkers.¹³ Residues 14-16 were not included as they were not resolved in the relevant crystal structure (PDB code 1YCR).

The initial structure of MDM2-peptide complex was taken from the crystal structure of p53 bound to MDM2 (PDB code 1YCR, resolved at 2.6Å).¹⁴ The structure used included residues 25–109 of the N-terminal domain of human MDM2 and residues 17–29 of the transactivation domain of p53. Orn(N₃) and stapled region of the peptides were modelled in the Xleap module in AMBER,¹⁵ RESP atomic charges for the stapled peptides were derived using the RED server.¹⁶ To keep the ends capped and neutral, the N- and C- termini of MDM2 were capped with acetyl (ACE) and N-methyl (NME) moieties respectively, while the N- and C-termini of the peptide were capped with acetyl (ACE) and amidate (NH₂) respectively. Molecular dynamics simulations were performed with the SANDER module of the AMBER11 package¹⁵ employing the all-atom ff99SB force field.¹⁷ Each system was simulated for 50 ns at constant temperature (300 K) and pressure (1 atm), and structures were stored every 10 ps. Simulations were carried out for the complexes of MDM2 with the p53 peptide, **SP0** and **SP1**. DSSP was used to calculate the secondary structures of the peptides.¹⁸ The simulation protocol was the same as reported earlier.¹⁹

The residues F19 to L25 of the transactivation domain (TA) of p53 form an α -helical segment, projecting the three hydrophobic side chains (F19, W23 and L26) on the same face of the helix;¹⁴ these 3 residues are also embedded into the hydrophobic cavity of the N-terminal domain of MDM2. Zondlo and coworkers have reported that the binding affinity of p53 for MDM2 increases when Pro at position 27 in p53 is replaced by Ser (P27S).²⁰ Extensive studies using molecular dynamics simulations have revealed that the constraint induced by the Pro27 on the backbone breaks the helicity at L25.²¹ However, upon mutation to Ser27, helicity is extended beyond L25. In order to increase the helicity of the peptide, we replace Pro27 with azido-ornithine Orn(N₃). Simulations show that this leads to increased helicity in both the unstapled and stapled peptides (Table S3). The increase in helicity is accompanied by the insertion of Leu26 (which is one of the key residues interacting with MDM2 [1]) deeper into the binding cavity in MDM2 increasing its contribution to the overall binding compared to p53 (data not shown) and a larger improvement in the interactions of W23 (Table 2).

Table S3. Helical propensity of p53 peptide and its unstapled and stapled analogs in their bound conformations

p53 ₍₁₇₋₂₉₎	% Helicity	SP0	% Helicity	SP1	% Helicity
E17	0.0	E	0.0	E	0.0
T18	0.0	T	0.0	T	0.0
F19	93.7	F	84.7	F	67.3
S20	99.4	Orn(N ₃)	99.6	Linker 1	98.3
D21	99.4	D	99.6	D	99.4
L22	98.4	L	99.8	L	99.4
W23	91.3	W	97.1	W	99.3
K24	78.8	R	99.1	R	96.5
L25	64.1	L	98.3	L	91.8
L26	0.0	L	97.6	L	88.8
P27	0.0	Orn(N ₃)	69.4	Linker 1	49.7
E28	0.0	E	37.9	E	23.6
N29	0.0	N	0.2	N	1.9

8. Confocal Microscopy

U2OS cells were seeded in an 8-chamber glass slide (20,000 cells/chamber in 250 μL). Cells were incubated at 37 °C in a 5 % CO_2 atmosphere for 24 h before the medium was removed, and new medium containing the fluorescent peptides (50 μM) was added. The cells were incubated for a further 24 hours before the medium was removed and they were washed with 100 μL PBS. The cells were fixed in 100 μL 4 % paraformaldehyde in PBS for 10 min, before being washed twice with 100 μL PBS. The chambers were then removed and a coverslip with mounting medium containing DAPI was applied. The cells were then imaged on a Zeiss LSM confocal microscope, using a 40 \times objective.

9. T22 Gene Reporter Assay

The gene reporter assay was conducted as we have previously described in the literature.¹²

10. References

1. Fischer, N. *et al.* Sensitivities of Some Imidazole-1-sulfonyl Azide Salts. *J. Org. Chem.* **77**, 1760–1764 (2012).
2. Hong, V., Presolski, S. I., Ma, C. & Finn, M. G. Analysis and Optimization of Copper-Catalyzed Azide–Alkyne Cycloaddition for Bioconjugation. *Angew. Chem. Int. Ed.* **48**, 9879–9883 (2009).
3. Kvach, M. V *et al.* Practical Synthesis of Isomerically Pure 5- and 6-Carboxytetramethylrhodamines, Useful Dyes for DNA Probes. *Bioconjugate Chem.* **20**, 1673–1682 (2009).
4. Pollock, J. B., Cook, T. R. & Stang, P. J. Photophysical and Computational Investigations of Bis(phosphine) Organoplatinum(II) Metallacycles. *J. Am. Chem. Soc.* **134**, 10607–10620 (2012).
5. Le Chevalier Isaad, A. *et al.* N α -Fmoc-Protected ω -Azido- and ω -Alkynyl-L-amino Acids as Building Blocks for the Synthesis of “Clickable” Peptides. *Eur. J. Org. Chem.* **2008**, 5308–5314 (2008).
6. Förster, B., Bertran, J., Teixidor, F. & Viñas, C. Synthesis of new arylcarboranes as precursors for oligomers. *J. Organomet. Chem.* **587**, 67–73 (1999).
7. Matsuda, K., Stone, M. T. & Moore, J. S. Helical Pitch of m-Phenylene Ethynylene Foldamers by Double Spin Labeling. *J. Am. Chem. Soc.* **124**, 11836–11837 (2002).
8. Tobe, Y. *et al.* m-Diethynylbenzene Macrocycles: Syntheses and Self-Association Behavior in Solution. *J. Am. Chem. Soc.* **124**, 5350–5364 (2002).
9. Bird, G. H., Bernal, F., Pitter, K. & Walensky, L. D. Chapter 22: Synthesis and Biophysical Characterization of Stabilized α -Helices of BCL-2 Domains. *Methods Enzymol.* **446**, 369–386 (2008).
10. Schon, O., Friedler, A., Bycroft, M., Freund, S. M. V & Fersht, A. R. Molecular Mechanism of the Interaction between MDM2 and p53. *J. Mol. Biol.* **323**, 491–501 (2002).
11. Miroux, B. & Walker, J. E. Over-production of Proteins in Escherichia coli: Mutant Hosts that Allow Synthesis of some Membrane Proteins and Globular Proteins at High Levels. *J. Mol. Biol.* **260**, 289–298 (1996).
12. Brown, C. J., Quah, S. T., Jong, J., Goh, A. M., Chiam, P. C., Khoo, K. H., Choong, M. L., Lee, M. A., Yurlova, L., Zolghadr, K., Joseph, T. L., Verma, C. S., Lane, D. P., *ACS Chem. Biol.* **8**, 506–512 (2012).
13. Bernal, F., Tyler, A. F., Korsmeyer, S. J., Walensky, L. D. & Verdine, G. L. Reactivation of the p53 Tumor Suppressor Pathway by a Stapled p53 Peptide. *J. Am. Chem. Soc.* **129**, 2456–2457 (2007).
14. Kussie P. H., Gorina S., Marechal V., Elenbaas B., Moreau J., Levine A. J., Pavletich. N. P. Structure of the MDM2 oncoprotein bound to the p53 tumor suppressor transactivation domain. *Science* **274**, 948–953 (1996).

15. Case D. A., Darden T., Cheatham III T. E., Simmerling C. L., Wang J., Duke R. E., Luo R., Walker R. C., Zhang W., Merz K. M., Roberts B., Wang B., Hayik S., Roitberg A., Seabra G., Kolossvary I., Wong K. F., Paesani F., Vanicek J., Liu J., Wu X., Brozell S. R., Steinbrecher T., Gohlke H., Cai Q., Ye X., Wang J., Heish M. J., Cui G., Roe D. R., Mathews D. H., Seetin M. G., Sagui C., Babin V., Luchko T., Gusarov S., Kovalenko A., Kollman P. A. **AMBER 11**, University of California, San Francisco (2010).
16. Vanquelef, E. *et al.* R.E.D. Server: a web service for deriving RESP and ESP charges and building force field libraries for new molecules and molecular fragments. *Nucleic Acids Res.* **39**, W511–W517 (2011).
17. Hornak, V. *et al.* Comparison of multiple Amber force fields and development of improved protein backbone parameters. *Proteins: Struct. Funct. Bioinf.* **65**, 712–725 (2006).
18. Kabsch, W. & Sander, C. Dictionary of protein secondary structure: Pattern recognition of hydrogen-bonded and geometrical features. *Biopolymers* **22**, 2577–2637 (1983).
19. Joseph, T. L., Madhumalar, A., Brown, C. J., Lane, D. P. & Verma, C. S. Differential binding of p53 and nutlin to MDM2 and MDMX: Computational studies. *Cell Cycle* **9**, 1167–1181 (2010).
20. Zondlo, S. C., Lee, A. E. & Zondlo, N. J. Determinants of Specificity of MDM2 for the Activation Domains of p53 and p65: Proline27 Disrupts the MDM2-Binding Motif of p53[†]. *Biochemistry* **45**, 11945–11957 (2006).
21. Dastidar, S. G., Lane, D. P. & Verma, C. S. Multiple Peptide Conformations Give Rise to Similar Binding Affinities: Molecular Simulations of p53-MDM2. *J. Am. Chem. Soc.* **130**, 13514–13515 (2008).